A theoretical study of the longitudinal motion of a vertical liquid jet

2001 J. Phys. A: Math. Gen. 34 6571

(http://iopscience.iop.org/0305-4470/34/34/304)

INSTITUTE OF PHYSICS PUBLISHING JOURNAL OF PHYSICS A: MATHEMATICAL AND GENERAL

J. Phys. A: Math. Gen. **34** (2001) 6571–6583 PII: S0305-4470(01)16411-5

A theoretical study of the longitudinal motion of a vertical liquid jet

H M Chung, J K Seok, S Y Moon[1] and C W Lee

Department of Mechanical Engineering, Kyungpook National University, 1370, San-kyuk dong, Puk-gu, Taegu, Korea

E-mail: symoon@knu.ac.kr

Received 15 August 2000, in final form 15 June 2001
Published 17 August 2001
Online at stacks.iop.org/JPhysA/34/6571

Abstract

The breakup phenomena of a vertical laminar jet issuing from a capillary tube in quiescent ambient air are investigated. Using a linear approach to the transient jet velocity, an approximate equation for the longitudinal motion of a vertical liquid jet is theoretically derived. The instability analysis is performed by a vibration method since the form of the equation resembles that of the Rayleigh differential equation in a dynamic system. From the dimensionless one-dimensional model, there are effects of the disturbance velocity on the instability in a gravity-free environment. In contrast, the instability of the liquid column is more affected by the disturbance velocity and the Bond number in a gravity environment, which is verified by comparisons of the theoretical data with the experimental frequencies. However, the effects of the surface wave are considered to be dominant in the condition of the large magnitude of initial disturbances by forces such as forced vibration

PACS numbers: 47.27.Wg, 02.30.-f, 47.20.-k

(Some figures in this article are in colour only in the electronic version)

1. Introduction

The major areas of current interest in the theoretical analysis of atomization are primarily the stability of liquid columns and the disintegration of liquid jets. This is why these topics have received a great deal of research attention. In a low-speed laminar jet, the causes of liquid column instability might be turbulence, cavitation, boundary layer and velocity relaxation effects. However, even though the overall jet integration is roughly understood, many details need to be explored to provide a complete description of the phenomenon.

[1] Corresponding author.

Rayleigh [1] carried out the first stability analysis for both inviscid and viscous cylindrical liquid columns in a vacuum. Weber [2] showed that the jet instability at high speed is affected by aerodynamic forces acting on the liquid–gas interface. The aerodynamic effects of a stationary liquid column in a moving gas stream were further investigated by Sterling and Sleicher [3] and were found to be responsible for an enhanced growth of varicose disturbances. In addition, Grant and Middleman [4] studied revised relations of Weber's theory into the breakup length. A low-viscosity liquid jet was also studied by Lafrance [5]. In contrast, the theory of Castleman [6] suggests that the spray phenomenon is a developed and disintegrated disturbance wave based on the interaction between the surface of the liquid column and the surrounding gas.

Another study on the aerodynamic instability of a liquid column was performed by Taylor and Levich [7]. The disintegration phenomenon of the Rayleigh breakup mode was investigated using a nonlinear numerical analysis method through the boundary element method [8]. Li and Shen [9] studied the convective instability. However, despite a large number of studies [10], they were insufficient to account for the breakup phenomenon since the effects of the dominant parameters associated with the breakup phenomenon are not regarded as significant causes of breakup.

The present study begins with the experimental assumption [13, 14] that the surface wave is exponentially increased as the axial component of the disturbance velocity in the liquid jet is increased at any point of the jet. The purpose of the present paper is to analyse the instability of a liquid column due to the growth of the surface wave, disturbance velocities, surface tension and gravity.

1.1. Review of Weber's theory

Weber's theory assumes that the radius of a liquid column R is disturbed by an axisymmetric perturbation δ with the variation in distance z from nozzle. The perturbation can be written as a Fourier series whose one component is of the form

$$\delta(z, t) = \eta_0 \exp(\alpha t + \mathrm{i}kz) \tag{1}$$

in which the growth rate α of the disturbance is calculated according to its wavenumber k. In other words, the disturbance to the radius is periodic along the z axis and it grows monotonically in time. η_0 is the initial amplitude of perturbation.

Furthermore, Weber assumes that the jet evolves in a vacuum or at a low speed and that both axial and radial stresses exerted by the surrounding environment can be disregarded. The equation has the form

$$\alpha^2 F_1 + \alpha F_2 \frac{3\mu\bar{k}^2}{\rho_{\mathrm{L}} R^2} = \frac{\sigma}{2\rho_{\mathrm{L}} R^3}(1 - \bar{k}^2)\bar{k}^2 \tag{2}$$

where μ is the viscosity of the liquid, ρ_L the liquid density, σ the surface tension and R the radius of the liquid column. $\bar{k}$ represents the dimensionless wavenumber kR, and F_1 and F_2 are ratios of Bessel functions whose arguments include both α and k. On the other hand, the general inviscid solution for growth rate α from Rayleigh instability analysis of the liquid jet is as follows:

$$\alpha^2 = \frac{\alpha k}{\rho R^2}(1 - k^2 R^2)\frac{I_1(kR)}{I_0(kR)} \tag{3}$$

where I_0 and I_1 are first- and second-order Bessel functions.

The growth rate α of the surface wave of the liquid column becomes the maximum growth rate $\alpha_{\max}$ when the radius of the liquid column R is equal to the amplitude of the disturbance

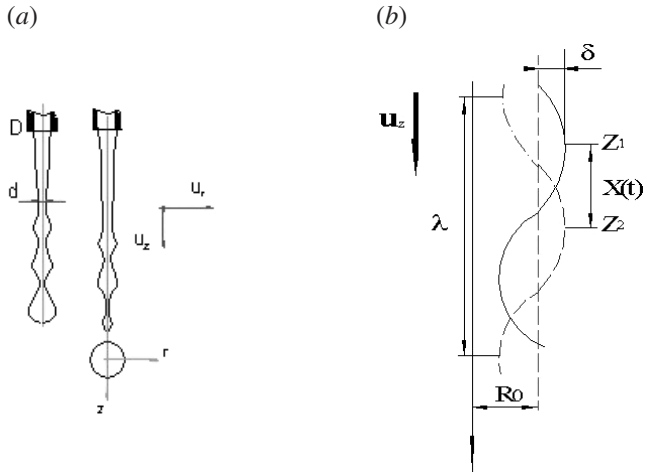

Figure 1. Schematic of a vertical liquid jet. (*a*) Breakup model. (*b*) Geometric configuration.

wave δ at the breakup time t_{BU}. That is to say

$$\delta(0, t_{\mathrm{BU}}) = R = \eta_0 \exp(\alpha_{\max} t_{\mathrm{BU}}). \tag{4}$$

If the jet is travelling at a constant speed U_0, the distance from the capillary exit at which the first drops appear is $L_{\mathrm{BU}} = U_0 t_{\mathrm{BU}}$. The breakup length L_{BU} can be expressed as the multiplication of the breakup time by the jet velocity, i.e.

$$L_{\mathrm{BU}} = \left(\frac{U_0}{\alpha_{\max}}\right) \ln\left[\frac{R}{\eta_0}\right]. \tag{5}$$

Another approach to the linear analysis of this is given by Lee [11] as a growth rate α parameter

$$\alpha^2 = \frac{\sigma}{2\rho R_0} \frac{4\pi^2}{\lambda^2} \left(1 - \frac{4\pi^2}{\lambda^2} R_0^2\right) \tag{6}$$

where λ is the wavelength of disturbance wave, ρ the liquid density, and R_0 the initial nozzle radius.

2. Formulation for a longitudinal vibration model

Consider a vertical liquid jet ejected from the nozzle. Figure 1 shows the breakup model and geometric configuration of a liquid column. The physical phenomenon can be solved by the Navier–Stokes systems with the continuity equation in the cylindrical coordinate system. In the present study, one-dimensional approximations to the equations for incompressible flows with constant transport properties are applied, based on the idea that the radial velocity is considerably small compared with the axial velocity in the cylindrical jet [12]. u_z is assumed to be the average axial velocity $u(z, t)$ across the radius [11]. The equations can be expressed as follows:

Continuity:

$$\frac{\partial u_z}{\partial z} + \frac{1}{r} \frac{\partial (r u_r)}{\partial r} = 0 \tag{7}$$

z momentum:

$$\rho\frac{\partial u_z}{\partial t}+\rho u_z\frac{\partial u_z}{\partial z}+\frac{\partial P}{\partial z}-\mu\frac{\partial^2 u_z}{\partial z^2}-\rho g_z=0. \tag{8}$$

Now it is supposed that the jet has the uniform velocity U_0, initial jet radius R_0 and wavelength λ just downstream in the capillary exit. Hence, the velocity of a vertical liquid jet can be written as

$$\begin{aligned} u_z &= u(z,t)=U_0+v(z,t)\\ &= U_0+u'(z)\frac{\mathrm{d}X}{\mathrm{d}t}=U_0+u'(z)\dot{X}(t) \end{aligned} \tag{9}$$

where t is the time, z the distance from the nozzle, U_0 the initial velocity of a liquid column, v the velocity of the disturbance, u' the axial component and the dimensionless magnitude of the disturbance velocity, and $\dot{X}$ a time component of the disturbance velocity.

The radius R of the liquid column can be written as

$$R(z,t)=R_0+\delta(z,t) \tag{10}$$

where $R_0(z)$ is the initial jet radius and $\delta(t,z)$ the amplitude of the disturbance wave of a liquid column. The continuity equation of (1) can be represented as

$$\frac{\partial R^2}{\partial t}+\frac{\partial(R^2u)}{\partial z}\Rightarrow\frac{\partial R}{\partial t}+u\frac{\partial R}{\partial z}+\frac{R}{2}\frac{\partial u}{\partial z}=0 \tag{11}$$

which is as derived by Lee [11].

For the inviscid jet, the pressure term is written in terms of the surface tension contribution as

$$p=\sigma\left(\frac{1}{R_\mathrm{N}}+\frac{1}{R_\mathrm{T}}\right). \tag{12}$$

From the geometric relation of the radius of curvature on the surface of a liquid column, the following expressions can be obtained:

$$R_\mathrm{N}=R\left[1+(\partial\delta/\partial z)^2\right]^{1/2} \tag{13}$$

$$R_\mathrm{T}=\frac{\left[1+(\partial\delta/\partial z)^2\right]^{3/2}}{-\partial^2\delta/\partial z^2}. \tag{14}$$

We suppose that the variation of the deviation δ of the radius from the value R_0 is a small change near the nozzle exit. Actually, the approximations can be found experimentally from a spectrum analysis [13, 14] and theoretically from the study of liquid jet dynamics [11]. These studies show that the variation of the amplitude spectrum of the disturbance δ abruptly increases only at the breakup region [13]. Hence, $\partial\delta/\partial z$ is a very small slope except for the breakup region.

For a small-amplitude disturbance, applying the assumption $(\partial\delta/\partial z)^2 \ll 1$ to equations (13) and (14) gives

$$\frac{1}{R_\mathrm{N}}\approx\frac{1}{R}=\frac{1}{R_0+\delta} \tag{15}$$

$$\frac{1}{R_\mathrm{T}}\approx-\frac{\partial^2\delta}{\partial z^2}. \tag{16}$$

When equations (15) and (16) are substituted into (12), the pressure term can be expressed as

$$p=\sigma\left(\frac{1}{R_0+\delta}-\frac{\partial^2\delta}{\partial z^2}\right). \tag{17}$$

Substituting equations (9) and (10) into (11) and integrating (11) with respect to t yields

$$\int \frac{\partial \delta}{\partial t}\,\mathrm{d}t + \int U_0 \frac{\partial \delta}{\partial z}\,\mathrm{d}t + \int u' \frac{\mathrm{d}X}{\mathrm{d}t}\frac{\partial \delta}{\partial z}\,\mathrm{d}t + \int \frac{R_0}{2}\frac{\mathrm{d}u'}{\mathrm{d}z}\frac{\mathrm{d}X}{\mathrm{d}t}\,\mathrm{d}t + \int \frac{\delta}{2}\frac{\mathrm{d}u'}{\mathrm{d}z}\frac{\mathrm{d}X}{\mathrm{d}t}\,\mathrm{d}t = 0. \tag{18}$$

Then

$$\delta - \delta_0 + \int U_0 \mathrm{i}k\delta\,\mathrm{d}t + \int u'\mathrm{i}k\delta\frac{\mathrm{d}X}{\mathrm{d}t}\,\mathrm{d}t + \frac{R_0}{2}\frac{\mathrm{d}u'}{\mathrm{d}z}X + \int \frac{\delta}{2}\frac{\mathrm{d}u'}{\mathrm{d}z}\frac{\mathrm{d}X}{\mathrm{d}t}\,\mathrm{d}t = 0. \tag{19}$$

Equation (1) can be written as the following, using Euler's identity:

$$\delta = \eta_0 \exp(\alpha t + \mathrm{i}kz) = A(t)\{\cos(kz) + \mathrm{i}\sin(kz)\} \tag{20}$$

where $A(t)$ is $\eta_0 \exp(\alpha t)$.

Substituting equation (20) into (19) and rearranging the terms according to the real part and imaginary part yields the following equation:

Real part:

$$(A - A_0)\cos(kz) - \int U_0 kA\sin(kz)\,\mathrm{d}t - \int u'kA\sin(kz)\frac{\mathrm{d}X}{\mathrm{d}t}\,\mathrm{d}t + \frac{R_0}{2}\frac{\mathrm{d}u'}{\mathrm{d}z}X + \int \frac{A}{2}\cos(kz)\frac{\mathrm{d}u'}{\mathrm{d}z}\frac{\mathrm{d}X}{\mathrm{d}t}\,\mathrm{d}t = 0. \tag{21}$$

Imaginary part:

$$(A - A_0)\sin(kz) + \int U_0 kA\cos(kz)\,\mathrm{d}t + \int u'kA\cos(kz)\frac{\mathrm{d}X}{\mathrm{d}t}\,\mathrm{d}t + \int \frac{A}{2}\sin(kz)\frac{\mathrm{d}u'}{\mathrm{d}z}\frac{\mathrm{d}X}{\mathrm{d}t}\,\mathrm{d}t = 0. \tag{22}$$

Rearranging equations (21) and (22) yields, respectively,

$$(A - A_0)\left[\cos(kz) - \frac{U_0 k}{\alpha}\sin(kz)\right] - \sqrt{a^2 + b^2}\sin(kz - \phi) \times \int A\frac{\mathrm{d}X}{\mathrm{d}t}\,\mathrm{d}t + \frac{R_0}{2}\frac{\mathrm{d}u'}{\mathrm{d}z}X = 0 \tag{23}$$

$$(A - A_0)\left[\sin(kz) + \frac{U_0 k}{\alpha}\cos(kz)\right] + \sqrt{c^2 + d^2}\sin(kz + \hat{\phi})\int A\frac{\mathrm{d}X}{\mathrm{d}t}\,\mathrm{d}t = 0 \tag{24}$$

where

$$\tan\phi = \frac{\frac{1}{2}\mathrm{d}u'/\mathrm{d}z}{u'k} = \frac{\beta u'}{2u'k} = \frac{\beta}{2k} \qquad a = u'k \quad b = \tfrac{1}{2}\mathrm{d}u'/\mathrm{d}z$$

$$\tan\hat{\phi} = \frac{u'ku}{\frac{1}{2}\mathrm{d}u'/\mathrm{d}z} = \frac{2u'k}{\beta u'} = \frac{2k}{\beta} \qquad c = u'k \quad d = \tfrac{1}{2}\mathrm{d}u'/\mathrm{d}z.$$

Combining equations (23) and (24) to eliminate the term $\int A\frac{\mathrm{d}X}{\mathrm{d}t}\,\mathrm{d}t$ produces

$$(A - A_0)\cos(kz - \widehat{\Pi}) = -\frac{R_0}{2}\frac{\mathrm{d}u'}{\mathrm{d}z}\frac{X}{\sqrt{\left(1 + \Pi\frac{U_0 k}{\alpha}\right)^2 + \left(\Pi - \frac{U_0 k}{\alpha}\right)^2}} \tag{25}$$

where

$$\frac{\sin(kz - \phi)}{\sin(kz + \hat{\phi})} = \Pi \qquad \tan\widehat{\Pi} = \frac{\Pi - \frac{U_0 k}{\alpha}}{1 + \Pi\frac{U_0 k}{\alpha}}.$$

If the imaginary part of equation (20) is deleted to attain the simplest analysis of jet [12], the real part of δ is $A(t)\cos(kz)$. Therefore, the left-hand side term of equation (25) is considered to be the real part of the disturbance amplitude term δ if the phase angle, $-\widehat{\Pi}$, approaches zero. At the same time, the right-hand side term of equation (25) becomes real if Π approaches zero. Equation (25) can be transformed into

$$\delta = \delta_0 - \frac{R_0}{2}\frac{\mathrm{d}u'}{\mathrm{d}z}\frac{X}{\sqrt{1+\left(\frac{U_0 k}{\alpha}\right)^2}} = \delta_0(z) - \Lambda\frac{\mathrm{d}u'}{\mathrm{d}z}X(t) \tag{26}$$

where

$$\Lambda(z) = \frac{R_0}{2\sqrt{1+\left(\frac{U_0 k}{\alpha}\right)^2}}.$$

Using Weber's theory as mentioned above, the disturbance amplitude $\delta(z,t)$ of a liquid column can be defined by equation (1) and the initial condition can be considered as

$$\begin{aligned} &\delta(z,t) : t = 0 \qquad \rightarrow \delta(z,0) = \delta_0 = \eta_0 \exp(\mathrm{i}kz) \\ &\delta(z,t) : z = 0, t = 0 \rightarrow \delta(0,0) = \delta_0(0,0) = \eta_0 \end{aligned} \tag{27}$$

where the initial longitudinal displacement $X(t)$ is

$$X(t) : t = 0 \rightarrow X(t) = 0. \tag{28}$$

The magnitude of the disturbance velocity, u' can be written as

$$u'(z) = \varsigma_0 \exp(\beta z) \tag{29}$$

where ς_0 and β represent the initial disturbance and the growth rate of the axial component of the disturbance velocity. Inserting equations (9), (17), (26) and (29) into (8) results in

$$\begin{aligned} \ddot{X} + U_0\frac{u'|_z}{u'}\dot{X} + u'|_z\dot{X}^2 - v\frac{u'|_{zz}}{u'}\dot{X} - \frac{g}{u'} + \frac{\sigma}{\rho u'}\frac{[k\eta_0\sin(kz) + \Lambda u'|_{zz}X]}{[R_0 + \eta_0\cos(kz) - \Lambda u'|_z X]^2} \\ -\frac{\sigma}{\rho u'}[k^3\eta_0\sin(kz) - \Lambda u'|_{zzzz}X] = 0 \end{aligned} \tag{30}$$

where the differential terms of u' are as follows:

$$u'|_z = \beta u' \qquad u'|_{zz} = \beta^2 u' \qquad u'|_{zzzz} = \beta^4 u'.$$

By examining the order of the sixth denominator term in equation (30), the equation can be further simplified due to the fact that the magnitude of the initial disturbance η_0 is too small to either see or detect during the experimental action. Thus, the assumption that $\eta_0/R_0 \ll 1$ is valid. The sixth denominator term can be expressed as follows:

$$R_0 + \eta_0\cos(kz) - \Lambda u'|_z X \approx R_0 - \Lambda u'|_z X. \tag{31}$$

Hence, equation (30) can be written as

$$\begin{aligned} \ddot{X} + U_0\beta\dot{X} + u'\beta\dot{X}^2 - v\beta^2\dot{X} - \frac{g}{u'} + \frac{\sigma}{\rho u'}\frac{[k\eta_0\sin(kz) + \Lambda u'\beta^2 X]}{[R_0 - \Lambda u'\beta X]^2} \\ -\frac{\sigma}{\rho u'}k^3\eta_0\sin(kz) + \frac{\sigma}{\rho}\Lambda\beta^4 X = 0. \end{aligned} \tag{32}$$

Equation (32) is a second-order nonlinear ordinary differential equation. From the parameters (ρ, σ, R_0, U_0) that characterize the jet, the following dimensionless variables can be determined

$$x \equiv \frac{X}{R_0} \qquad t* \equiv \frac{t}{\sqrt{\rho R_0^3/\sigma}}. \tag{33}$$

The following result of the sixth denominator term can be arranged from equation (26):

$$-\Lambda u'\beta X = \delta - \delta_0. \tag{34}$$

As we noted earlier, we assume that the variation in the perturbation δ is considerably small along the nozzle exit. According to equations (1) and (27), the difference between δ and δ_0 is significantly small, compared with R_0:

$$R_0 - \Lambda u'\beta X = R_0 + \delta - \delta_0 \approx R_0. \tag{35}$$

Hence, equation (32) can be simplified in a dimensionless form

$$\ddot{x} + \beta R_0\left(\sqrt{\mathrm{We}} - \beta R_0 \mathrm{Oh}\right)\left[1 + \frac{u'}{(\sqrt{\mathrm{We}} - \beta R_0 \mathrm{Oh})}\dot{x}\right]\dot{x} + \Lambda R_0\beta^2(1 + R_0^2\beta^2)x + \frac{(1 - k^2R_0^2)}{u'}k\eta_0 \sin(kz) - \frac{\mathrm{Bo}}{u'} = 0 \tag{36}$$

where

$$\text{Weber number:} \quad \mathrm{We} = \frac{\rho U_0^2 R_0}{\sigma}$$

$$\text{Ohnesorge number:} \quad \mathrm{Oh} = \frac{\mu}{\sqrt{\sigma R_0 \rho}}$$

$$\text{Bond number:} \quad \mathrm{Bo} = \frac{\rho g R_0^2}{\sigma}.$$

The form of equation (36) is

$$\ddot{x} + a(1 + b\dot{x})\dot{x} + w_n x + s = 0 \tag{37}$$

which is similar to the Rayleigh equation. The instability condition is determined based on whether the coefficient, $a(1 + b\dot{x})$, of the damping term is less than zero. For an inviscid fluid ($\mu = 0$), $\beta R_0 \mathrm{Oh} \approx 0$. The coefficient of the damping term in equation (37) is

$$\dot{x} = -\frac{\sqrt{\mathrm{We}}}{u'}. \tag{38}$$

Combining equations (33) and (38) yields

$$\frac{v}{U_0} = -1. \tag{39}$$

From equations (9) and (39), u becomes zero. Physically, this means that there exists a force acting in opposition to the axial direction at a breakup time.

Therefore, the initial conditions and the boundary condition are

$$\dot{x}(0) = x(0) = 0 \qquad \dot{x}(t^*_{\mathrm{BU}}) = -\frac{\sqrt{\mathrm{We}}}{u'}. \tag{40}$$

Differentiating equation (37) with respect to t^* produces

$$x + a(1 + 2b\dot{x})\ddot{x} + w_n\dot{x} = 0 \tag{41}$$

which does not involve gravity terms.

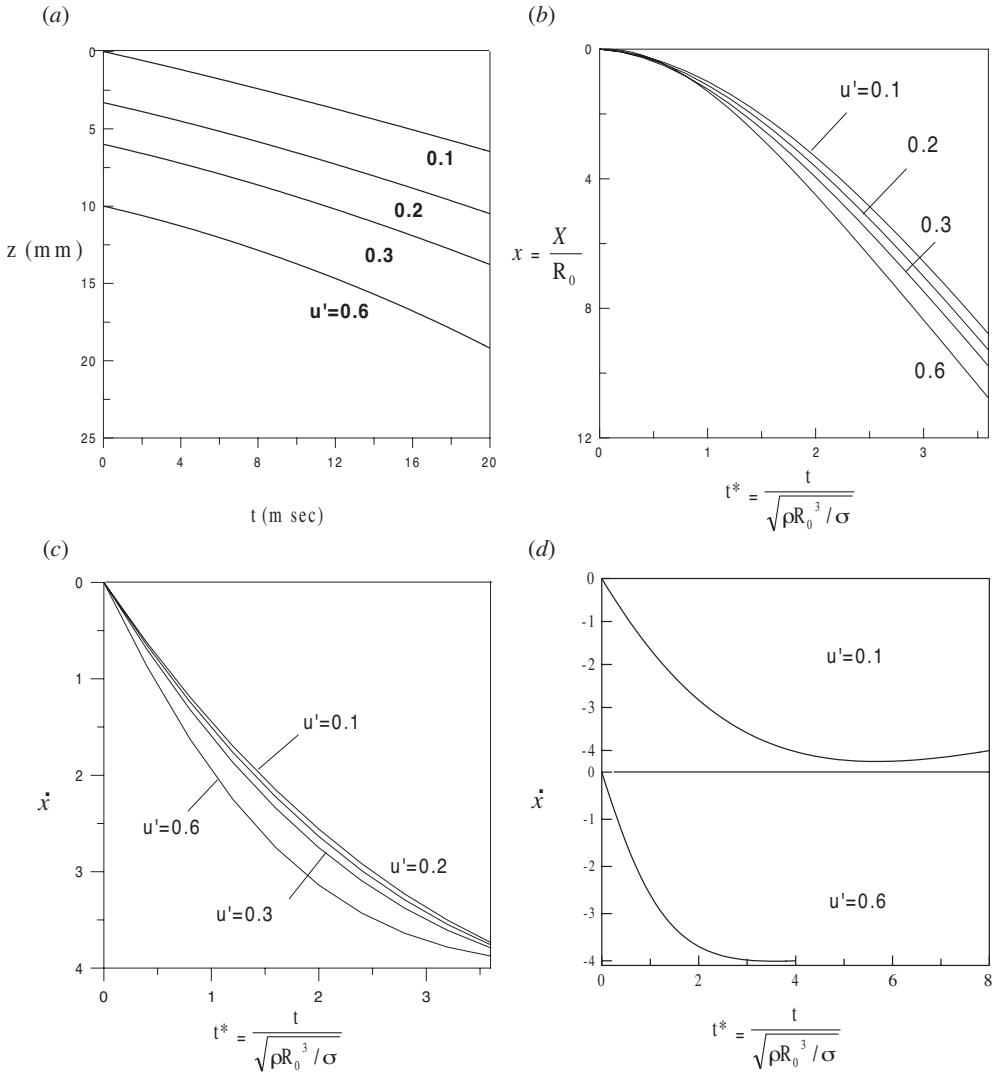

Figure 2. Distributions of characteristics with the variation in u' in a gravity-free environment. (*a*) Distributions of the dimensional position with the variation in u'. (*b*) Distributions of the dimensionless displacement with the variation in u'. (*c*) Distributions of a dimensionless time component of the disturbance velocity with the variation in u'. (*d*) Occurrence of breakup with the increase in u'.

3. Discussions and results

Numerical investigations were performed into distributions of characteristics with the variations in u' and s in gravity-free and gravity environments to warrant the formulations of the breakup model. Water at a temperature of 22 °C is utilized as a working fluid. The fourth-order Runge–Kutta method is used in solving the ordinary differential equations.

Figure 2 denotes the solutions of equation (37) for the gravity-free environment using the boundary conditions in equation (40). The calculations are performed under the assumption that the working fluid is water. The distributions of the longitudinal position according to

the changes in u' are shown in figure 2(a). In this figure, the large value of u' equates to an increase in the distance from the nozzle since u' is a function of the distance z in equation (29) in regards to the small initial disturbance ς_0 of u'. Note that the location in which u' is 0.1 indicates the position near the nozzle. On the other hand, the distance at 8 mm away from the nozzle represents the place of $u' = 0.6$ where a drop is on the verge of breaking up. Figure 2(a) indicates that the distributions of the longitudinal position form similar shapes, respectively, at different distances from the nozzle. This indicates that with increase in u', wavelengths are increased slightly. Figure 2(b) shows distributions of the dimensionless axial displacement with the variation in u' and time. Changes in u' represent those of the initial disturbance ς_0 at the same position of z. The axial displacement of the surface wave is slightly increased with respect to time as the initial disturbance ς_0 increases. In other words, there is a small effect of the initial disturbance ς_0 on the instability in a gravity-free environment. Figure 2(c) demonstrates the distributions of a time component of the disturbance velocity according to changes in the initial disturbance ς_0 of u' at the same position. These changes of the disturbance velocity v increase gradually as the changes in the initial disturbance ς_0 of u' increase. It is recognized in figure 2(d) that the breakup occurs at $t^* = 4$ since there is no variation in the disturbance velocity $\dot{x}$ with respect to changes in time.

When equation (36) is compared with equation (37), the parameter s can be written as

$$s = \frac{(1 - k^2 R_0^2)}{u'} k\eta_0 \sin(kz) - \frac{Bo}{u'} \tag{42}$$

which plays a role in increasing the instability. Moreover, the first term of equation (42) has the dimensionless parameter kR_0 which affects the instability of the liquid jet, depending on whether $kR_0 < 1$ or $kR_0 \geqslant 1$. In the areas in which the surface wave increases, that being when η_0 is large, the profile of the surface wave disturbance follows a sine curve according to the distance z from the nozzle. If the order of magnitude of the initial disturbance η_0 of the surface wave is considerably small, the parameter s can be expressed as the ratio of Bond number to u'. Thus, s is inverse to the distance z from the relation $s \approx \mathrm{Bo}/u'$.

Figure 3 shows the distributions of characteristics for different values of the parameter s in a gravity environment. In figure 3(a), the dotted and solid curves represent the trajectories of the points on the surface wave depending, respectively, on whether the magnitude of disturbance velocity u' is constant or not. Figure 3(a) shows how the distributions of the solid curves have similar tendencies with the variation in s compared with those found in figure 2(a) where the parameter s is neglected. However, the trajectory of $s = 0.28$ is different from the actual trajectory which would be the dotted line of $s = 1.7$. The difference of the wavelength is due to the effect of the Bond number. The distributions of the disturbance displacement and the time component of the disturbance velocity increase at the same position as s increases as shown in figures 3(b) and (c). Figure 3(b) shows how the surface wave is elongated with an increase in the Bond number. This can be also ascribed to how the Bond number is proportional to the volume which is that of the pendent drop just before a part of that drop falls away from the nozzle [12]. This could also be attributed to how the elongation of the surface wave is increased as the weight of the pendent drop is increased. Figure 3(c) demonstrates that the effects of the Bond number become larger as the disturbance velocity v becomes larger. This can be explained by the fact that the disturbance velocity is accelerated due to the increase in the weight of the pendent drop. However, the contribution of the surface wave to the dimensionless parameter s may be considered to be dominant in the condition of the large magnitude of the initial disturbance η_0, such as the forced vibration.

The high-speed photographs taken at intervals of 400 Hz under the same condition as the calculated case are shown in figure 4. The solid and dotted curves as shown in figure 3(a) are compared with the trajectories of the points in the experiment. It is found that the actual

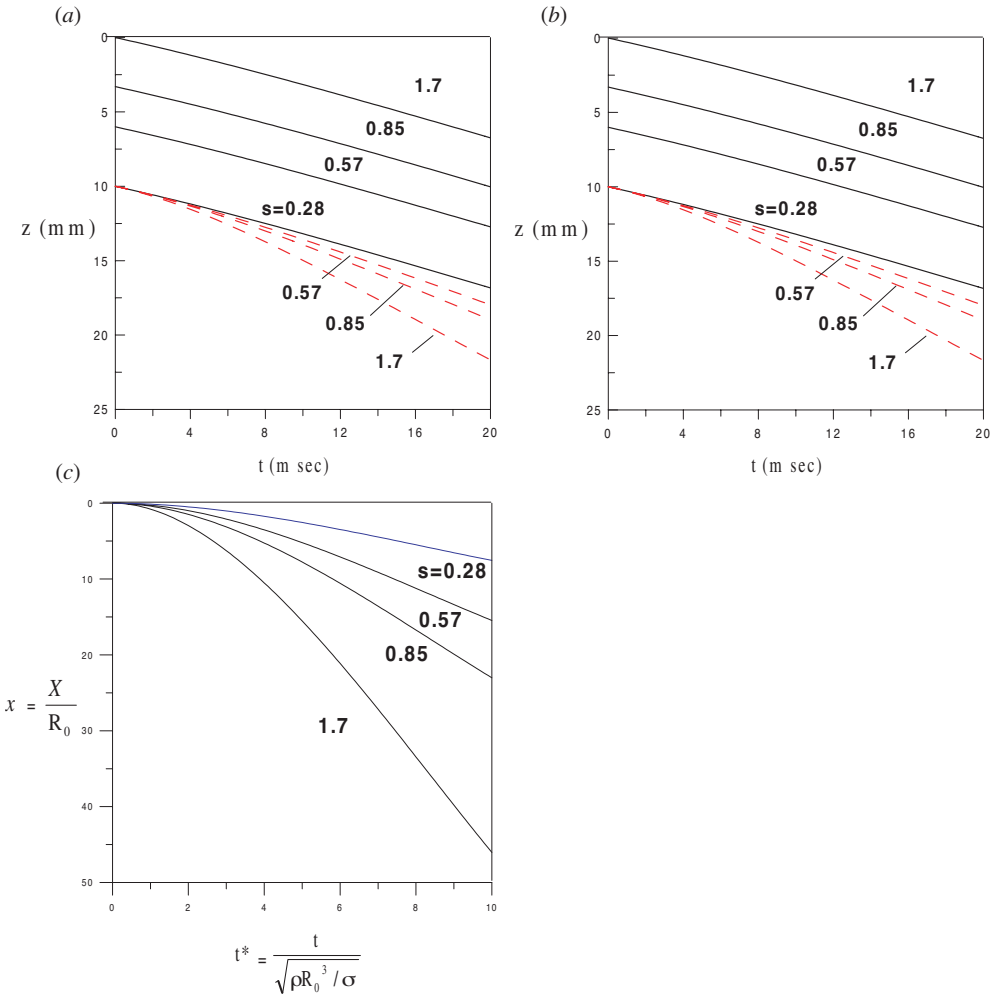

Figure 3. Distributions of characteristics with the variation in parameter s in a gravity environment. (a) Distributions of trajectories at different positions (solid curves) and same positions (dotted curves) with the variation in s. (b) Distributions of the dimensionless displacement with the variation in s at the same position. (c) Distributions of a dimensionless time component of the disturbance velocity with the variation in s at the same position.

phenomena in figure 4 are similar to profiles of the solid curves of the surface waves according to the changes of u'. The picture shows that the thin dotted line would be the trajectory in a gravity-free environment. However, the actual trajectory in a gravity environment is represented by the thick dotted line. The difference of wavelength is due to the Bond number. It is observed in figure 4 that as water issues vertically from a capillary with an inside diameter D of 2.2 mm, the wavelength shows λ_{BU} of 10 mm during 20 ms where λ_{BU} agrees well with the Rayleigh or Weber theory [1, 2]: $\lambda_{BU} \approx 4.51D$.

Note that the wavelength of the surface wave almost did not change with the variation of u' near the nozzle exit, this being the physical phenomenon occurring in the gravity-free environment.

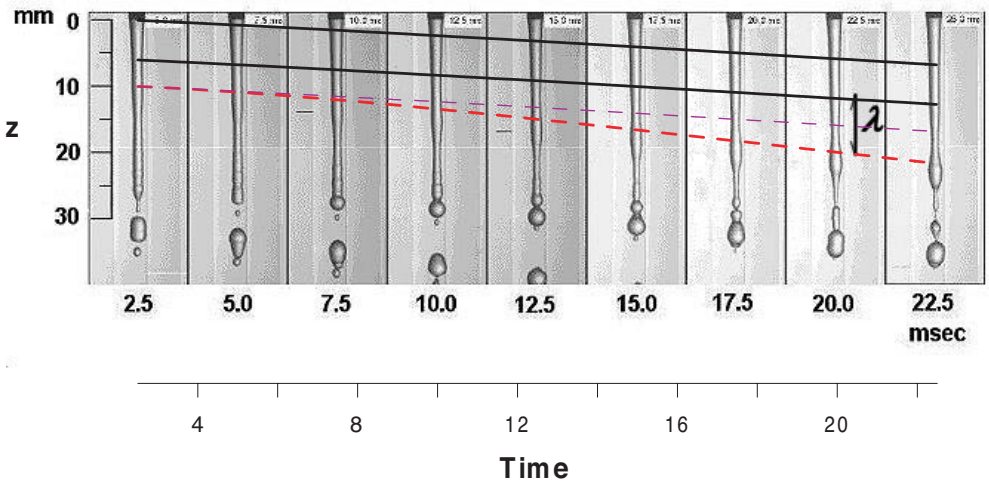

Figure 4. Comparisons of the theoretical data figure 3(*a*) with high speed photographs taken at the photographic interval of 400 Hz (at the break-up interval of 50 Hz).

Therefore, the variation of the Bond number plays a dominant role in increasing the wavelength of the vertical jet near breakup point. The pendent drop moves 10 mm downward during 20 ms at the breakup region as shown in figure 4, meaning that at this position the pendent drop is more subject to Bond number effects than at any other position.

Figure 5 demonstrates the experimental frequencies of surface waves on a liquid column, thus presenting comparisons of the experimental data with the theoretical data. Figure 5(*a*) shows the frequency spectra at various positions from the nozzle exit. Figure 5(*b*) shows the monotone contour intensity expression of the spectrum obtained from figure 5(*a*). The circle marks indicate the theoretical frequencies with respect to z while the solid curves denote the fitting curve of the frequencies obtained using the theoretical frequencies data. The curve of the theoretical frequencies falls within the experimental frequency spectrum [14] ranging from 20 and 80 Hz at the breakup point $z = 20$ mm.

4. Conclusions

In this paper, a theoretical model of a liquid jet for the absence of aerodynamic effects in the Rayleigh instability region has been obtained. A longitudinal model of the jet somewhat resembles that of the Rayleigh ordinary differential equation in a dynamic system. In a gravity-free environment, the wavelength increases with the increase of u'. Distributions of the trajectories in a gravity environment have similar tendencies to the variation in s compared with those in a gravity-free environment. When on the verge of breaking up, wavelengths between the gravity and gravity-free environments vary due to the effects of the Bond number. The result is verified comparing the analytical solution of a dimensionless 1D model of the liquid jet column with the picture taken and experimental data. The instability of the jet in the laminar flow region is more affected by the disturbance velocity, the initial disturbance of the jet and Bond number than by any other factors. However, the surface effects can be considered to be dominant in the large magnitude condition of the initial disturbance by forces such as forced vibration.

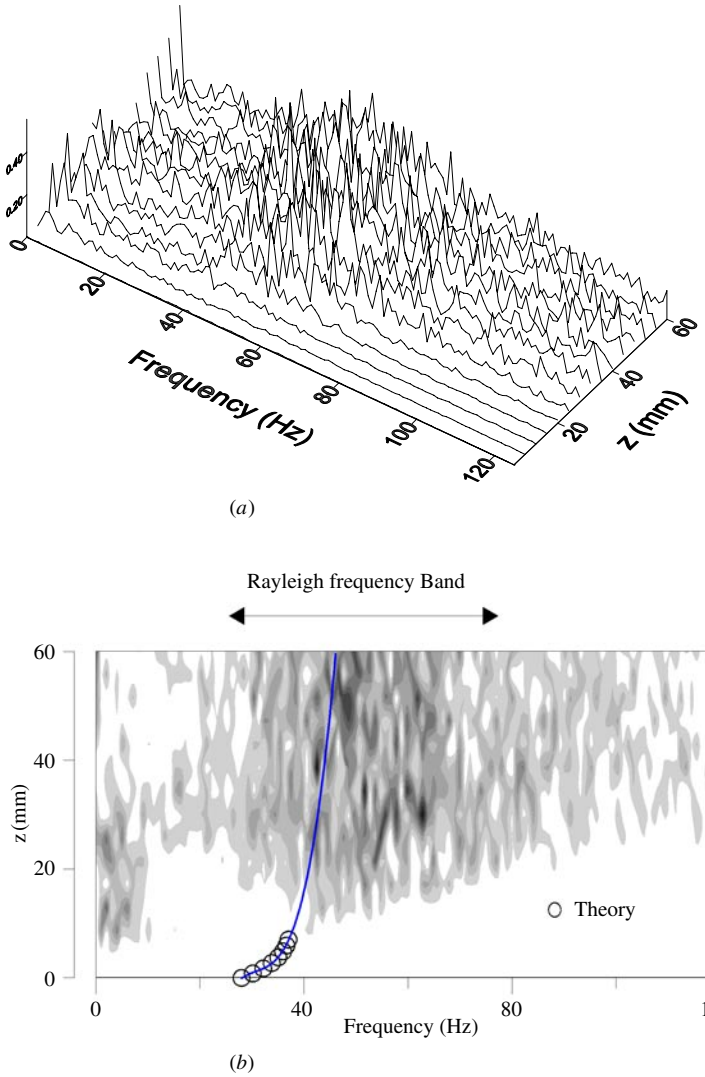

Figure 5. Experimental frequencies of surface waves on liquid column. (*a*) Spectrum structure of surface waves on liquid column. (*b*) Monotone intensity of the spectrum.

References

[1] Rayleigh L 1879 On the instability of jets *Proc. Lond. Math. Soc.* **10** 4–13
[2] Weber C 1931 Zum zerfall eines flussigkeitstrahles *Z. Angew. Math. Mech.* **11** 136–59
[3] Sterling A M and Sleicher C A 1975 The instability of capillary jets *J. Fluid Mech.* **68** 477–95
[4] Grant R P and Middlenman S Newtonian jet stability *ALChE J.* **12** 669–78
[5] Lafrance P 1975 Nonlinear breakup of a laminar liquid jet *Phys. Fluids* **18** 428
[6] Castleman R A 1932 The mechanism of atomization accompanying solid injection *Report 440* National Advisory Committee for Aeronautics pp 735–46
[7] Levich V G 1962 *Physico-Chemical Hydrodynamics* (Englewood Cliffs, NJ: Prentice-Hall)
[8] Hilbing J H, Heister S D and Spangler C A 1995 A boundary-element method for atomization of a finite liquid jet *Atomiz. Sprays* **5** 621–38

[9] Xianguo Li and Jihua Shen 1988 Absolute and convective instability of cylindrical liquid jets in Co-flowing gas streams *Atomiz. Sprays* **8** 45–62
[10] Siringanao W A and Mehring C 2000 Review of theory distortion and disintegration of liquid stream *Prog. Energy Combust. Sci.* **26** 609–55
[11] Lee H C 1974 Drop formation in a liquid jet *IBM J. Res. Dev.* **18** 364
[12] Middlemann S 1995 *Modeling Axisymmetric Flows* (New York: Academic) pp 112–22
[13] Arai M and Amagai K 1999 Surface wave transition before breakup on laminar liquid jet *J. Heat Fluid Flow* **20** 507–12
[14] Suk J K, Chung H M and Lee C W A study on gravity force effect of breakup mechanism in liquid jet *Ilass-Asia 99 (Yongin, South Korea)* pp 73–8
[15] Hilbing J H, Heister S D and Spangler C A 1995 A boundary element method for atomization of a finite liquid jet *Atomiz. Sprays* **5** 621–38